METEOROLOGICAL SERVICE

TECHNICAL NOTE No. 48

NUMERICAL FORECASTING USING LAPLACE TRANSFORMS: THEORY AND APPLICATION TO DATA ASSIMILATION.

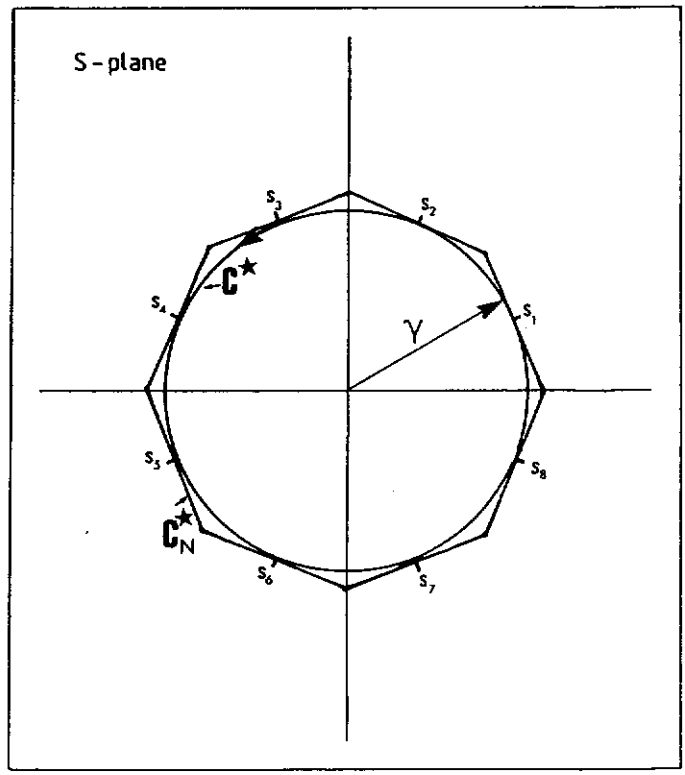

By
Peter Lynch M.Sc., Ph.D.

UDC 551.509.313

Price £2.20

GLASNEVIN HILL, DUBLIN 9
JULY 1986

NUMERICAL FORECASTING USING LAPLACE TRANSFORMS: THEORY AND APPLICATION TO DATA ASSIMILATION.

Abstract

The Laplace Transform technique is used to develop a numerical scheme for integrating the primitive equations. The scheme is capable of faithfully simulating the dynamics of the low frequency components of the flow, whilst the high frequency components are strongly attenuated. Thus, it models the meteorologically significant synoptic flow, uncontaminated by gravity wave noise.

The Laplace Transform (LT) method has been compared to a standard Adams Beshforth (AB) method in the context of a one dimensional model. The LT method with a one hour timestep gives results very similer to the AB scheme with a 30 second step. The scheme is subject to a stability criterion similer to that of the semi-implicit method, and depending on the advection velocity. If the advection is integrated in a Lagrangian manner this restriction is relexed.

The Laplace transform method is particularly suitable for insertion of data during an integration: since the gravity waves are strongly damped, the model can absorb the inserted information without undue shock. Other schemes generally require reinitialization after data insertion, or else the imposition of strong divergence damping. Thus, the method would appear to be a useful means for continuous data assimilation.

TABLE OF CONTENTS

1. INTRODUCTION

The main objective of Numerical Weather Prediction (NWP) is to provide accurate guidance on the development of synoptic weather systems evolving from a specified initial state. The basic equations of current NWP models — the *primitive equations* — have been found to be capable of faithfully simulating the dynamics of these systems. However, these equations also have high frequency solutions corresponding to gravity waves. These are of little meteorological importance, but they cause computational and other problems, and are generally regarded as undesirable *noise*.

We can deal with gravity wave noise in two ways. Historically, the first method was to modify the equations of motion so that the only solutions remaining were the low frequency meteorological motions. The resulting filtered equations — the quasi-geostrophic equations — were used successfully for the first computer forecasts, and are noise-free. However, they involve approximations which are not always justified, with consequent errors in the forecasts. Therefore, the primitive equations are generally used nowadays for NWP, and the corruption of forecasts by noise is prevented by imposing balance conditions on the initial fields. This process is called initialization.

Properly initialized fields result in smoothly evolving flow patterns during the forecast, provided that the integration proceeds undisturbed. If we wish to modify the fields during the integration, e.g. to correct them in the light of new observational data, the balance may be disturbed and noise generated. Again, we may prevent this in two ways: the fields may be reinitialized after data insertion, or a numerical scheme may be chosen which prevents or suppresses noise. The reinitialization of the fields may be computationally expensive, particularly if data is being assimilated at frequent intervals. Therefore, we consider in this report a scheme which suppresses noise by allowing the low frequency motions to evolve uninhibited while strongly damping the high frequency motions.

A solution method using the Laplace transform technique was developed by Lynch (1985a) and applied to the problem of initialization. In the present study the same method is used to devise a numerical scheme for integrating the equations of motion. The method forecasts the low frequency motions while the high frequency components are strongly attenuated. The method is compared to a well-tried Adams Bashforth method in the context of a simple one-dimentional model. Both methods give very similar forecasts of the rotational component of the flow. The evolution of the divergence is much smoother for the Laplace transform method.

The stability properties of the Laplace transform method are considered. The approximation of the inversion integral by a sum introduces an error; this has been investigated by Van Isacker and Struylaert (1985). Their results can be used to derive a stability criterion for the maximum allowable timestep. It turns out to be a very lenient and easily satisfied condition. The practical limit on timestep arises through the nonlinear advection terms: the stability condition is the same as that resulting from the semi-implicit scheme, and depends on the maximum advection velocity. This restriction can be circumvented by the use of a Lagrangian treatment of advection, resulting in a practically unrestricted scheme.

The Laplace transform scheme is of particular interest in the context of continuous data assimilation. This process involves the modification of the meteorological fields during a forecast run by insertion of new data. One consequence of data insertion is the disruption of the fine balance between the fields, resulting in spurious gravity wave noise. Since frequent reinitialization is impractical, the noise must be eliminated in some other way. Most methods of damping, such as divergence damping, which are designed to control high frequency waves, also affect the rotational motions, altering the forecast. The Laplace transform technique specifically selects the high frequency gravity wave components for elimination, and leaves the meteorological motions virtually unaffected. As a result, data may be inserted continuously and assimilated by the model without undue shock. Parallel runs using the Adams Bashforth (AB) and Laplace transform (LT) schemes for data

assimilation show that the latter scheme absorbs inserted data without appreciable noise in the ensuing forecast. The AB scheme suffers from noticeable residual noise even when the fields are reinitialized after data insertion.

The Laplace transform scheme bears a close resemblance to a scheme using normal modes, proposed by Daley (1980). Both methods forecast the slowly varying rotational components of the flow while diagnosing appropriate gravity wave components. Since the LT scheme does not require explicit knowledge of the model normal modes, it may be more useful in the context of limited area modelling. Both methods involve costly transformations between physical space and normal mode or image space. It is possible to derive a set of equations in physical space (I call them the *slow equations*) with properties similar to the scheme of Daley, but avoiding transformations at each timestep. It is proposed that these equations would provide an efficient and effective method for forecasting the meteorologically significant components of the flow and for continuous data assimilation.

2. THE LAPLACE TRANSFORM METHOD

In this section we describe the Laplace transform method of integrating the equations of motion. In section 2a we outline the theory of the method; section 2b deals with the effects of discretization of the inversion operator; and in section 2c we consider the question of stability. The numerical model used in this study is outlined in section 2d.

2a. Theory.

We consider a system whose state at time t is specified by the vector $\mathbf{X}(t)$, which is governed by an equation of the form

$$\frac{d\mathbf{X}}{dt} + \mathbf{L}\mathbf{X} + \mathbf{N}(\mathbf{X}) = \mathbf{0} \qquad (2\cdot1)$$

where $\mathbf{L}$ is a linear operator and $\mathbf{N}$ a nonlinear vector function. If the system is in the state $\mathbf{X}^0$ at time $t = 0$ then the Laplace transform of this equation is

$$\mathbf{M}\hat{\mathbf{X}} + \hat{\mathbf{N}} = \mathbf{X}^0 \qquad (2\cdot2)$$

where $\mathbf{M}(s) = (s\mathbf{I}+\mathbf{L})$ with $\mathbf{I}$ the identity matrix, s is the transform variable and carets denote Laplace transforms.

If we consider the evolution of the system over a short time interval $(0,\Delta t)$, and assume that the nonlinear term does not vary, we may solve (2·2) as follows

$$\hat{\mathbf{X}} = \mathbf{M}^{-1}[\mathbf{X}^0 - \mathbf{N}^0/s] \qquad (2\cdot3)$$

where $\mathbf{N}^0 = \mathbf{N}(\mathbf{X}^0)$. Then, to find the solution at time $t = \Delta t$ we apply the inverse Laplace transform

$$\mathbf{X}(\Delta t) = \mathcal{L}^{-1}\left\{\mathbf{M}^{-1}[\mathbf{X}^0 - \mathbf{N}^0/s]\right\}\Big|_{t=\Delta t}$$

If we are interested only in the slowly varying components of the flow we may replace $\mathcal{L}^{-1}$ by the modified inverse $\mathcal{L}^{*}$ (see Appendix) which acts to filter out the high frequency components:

$$\mathbf{X}^1 = \mathbf{X}^*(\Delta t) = \mathcal{L}^*\left\{ \mathbf{M}^{-1}[\mathbf{X}^0 - \mathbf{N}^0/s] \right\} \Big|_{t=\Delta t} \tag{2·4}$$

Having the solution at $t = \Delta t$ we may proceed stepwise to extend the forecast. However, it is better to employ a leapfrog timestepping technique; thus, the solution $\mathbf{X}^2$ at time $2\Delta t$ can be approximated by

$$\mathbf{X}^2 = \mathcal{L}^*\left\{ \mathbf{M}^{-1}[\mathbf{X}^0 - \mathbf{N}^1/s] \right\} \Big|_{t=2\Delta t}$$

where $\mathbf{N}^1 = \mathbf{N}(\mathbf{X}^1)$ is evaluated at the centre of the interval $(0, 2\Delta t)$. In general, having the solutions $\mathbf{X}^{n-1}$ and $\mathbf{X}^n$ at times $(n-1)\Delta t$ and $n\Delta t$, we advance the solution to time $(n+1)\Delta t$ as follows:

$$\mathbf{X}^{n+1} = \mathcal{L}^*\left\{ \mathbf{M}^{-1}[\mathbf{X}^{n-1} - \mathbf{N}^n/s] \right\} \Big|_{t=2\Delta t} \tag{2·5}$$

Here the origin of time for the inverse transform is $(n-1)\Delta t$ so that $\mathbf{X}^{n-1}$ is the 'initial condition', and the nonlinear terms are evaluated at the centre of the interval.

An alternative timestepping scheme was proposed by Van Isacker and Struyleert: We assume that the solutions at $n\Delta t$ and $(n+\frac{1}{2})\Delta t$ are $\mathbf{X}^n$ and $\mathbf{X}^{n+\frac{1}{2}}$. Then we make two steps as follows:

$$\mathbf{X}^{n+1} = \mathcal{L}^*\left\{ \mathbf{M}^{-1}[\mathbf{X}^n - \mathbf{N}(\mathbf{X}^{n+\frac{1}{2}})/s] \right\} \Big|_{t=\Delta t} \tag{2·6a}$$

$$\mathbf{X}^{n+3/2} = \mathcal{L}^*\left\{ \mathbf{M}^{-1}[\mathbf{X}^n - \mathbf{N}(\mathbf{X}^{n+\frac{1}{2}})/s] \right\} \Big|_{t=3\Delta t/2} \tag{2·6b}$$

The nonlinear terms are calculated only once. This scheme is also started by a forward step. Unlike the leapfrog method, it has no computational mode. We refer to this method as the *two-step scheme*.

2b. *Discretization of the Inverse Transform*

We have defined the modified inverse transform

$$f^*(t) = \Sigma^* \{ \hat{f} \} = \frac{1}{2\pi i} \oint_{C^*} e^{st} \hat{f}(s) \cdot ds \qquad (2\text{-}7)$$

To evaluate Σ^* numerically, we replace the circular contour C^* by a circumscribed regular N-gon C_N^* (see Figure 1). The integrand is evaluated at the midpoints s_n of the edges of C_N^*:

$$s_n = \gamma \exp[(2n-1)i\pi/N]$$

Now consider the number s_n raised to the power $k = m+rN$ where $0 \le m < N$. We can easily show that

$$s_n^k = (-\gamma^N)^r \cdot s_n^m$$

Thus, the function s_n^k (*qua* function defined on C_N^*) *looks like* the function s_n^m multiplied by a constant $(-\gamma^N)^r$. This *aliasing* means that only the first N powers of s_n are linearly independent:

$$\{ s_n^0, s_n^1, s_n^2, \cdots, s_n^{N-1} \}$$

is a basis for functions defined on C_N^*. Thus, we truncate Taylor series expansions after N terms, so the exponential function e^{st} is replaced by

$$e_N^{st} = \sum_{m=0}^{N-1} (st)^m/m! \qquad (2\text{-}8)$$

The discrete modified inverse Laplace transform is now defined as follows

$$\Sigma_N^* \{ \hat{f} \} \Big|_t = \frac{(1/\kappa)}{2\pi i} \sum_{n=1}^{N} \hat{f}(s_n) e_N^{s_n t} \cdot \Delta s_n. \qquad (2\text{-}9)$$

(where the correction factor $\kappa = (\tan(\pi/N))/(\pi/N)$ is discussed in Lynch,

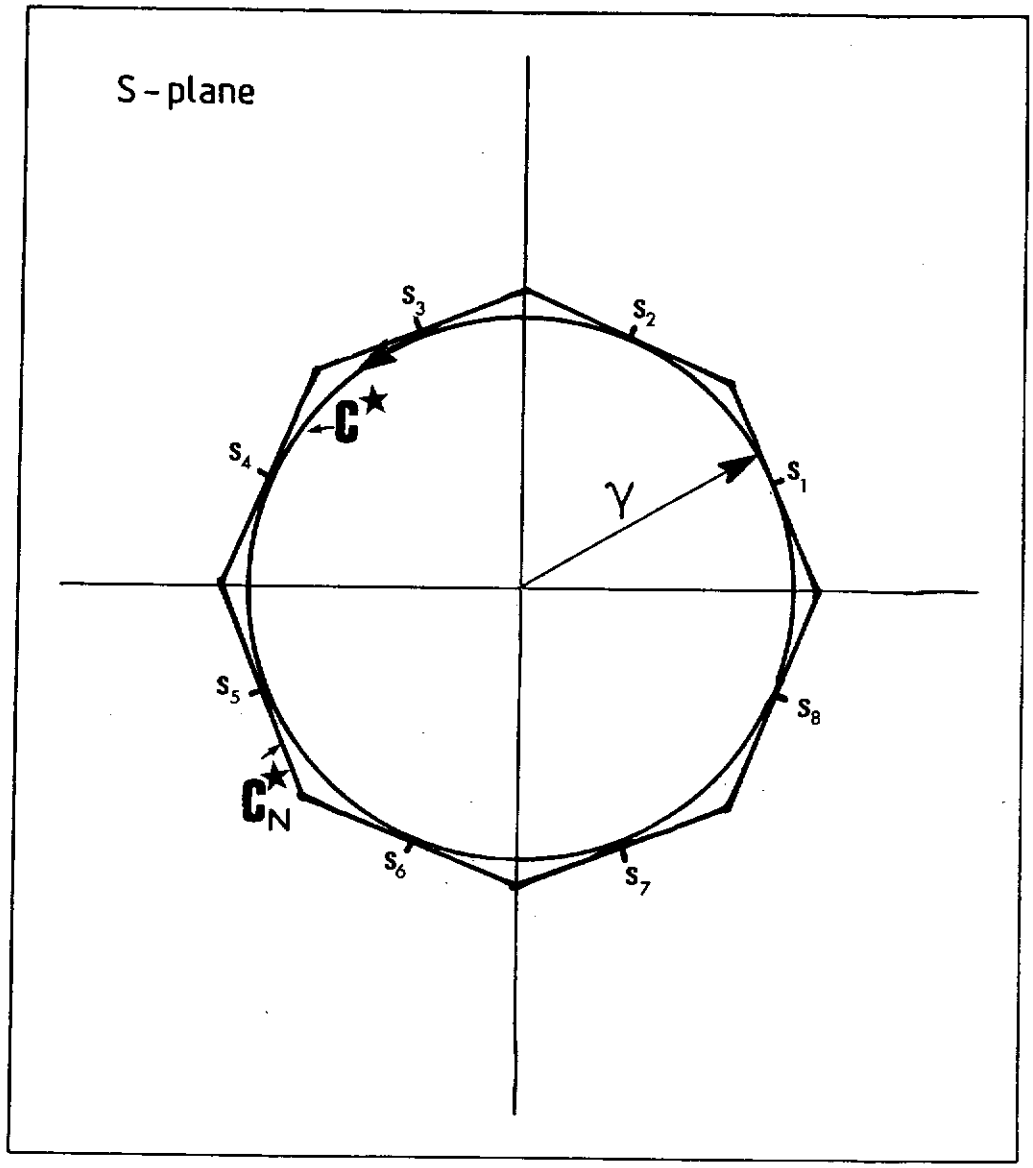

Figure 1.

1985b). Using the fact that $\Delta s_n/s_n = 2\pi i \cdot \kappa/N$ we can rewrite this transform as

$$\boxed{\Sigma_N^*\{\hat{f}\}\,|_t = \frac{1}{N}\sum_{n=1}^{N}\hat{f}(s_n)e_N^{s_n t}\cdot s_n.} \qquad (2\cdot 10)$$

(this is the form used by Van Isacker and Struyleert, 1985). We have shown in Lynch (1985a) that $\Sigma^*\Sigma$ is a perfect low-pass filter (see also the Appendix). It is of interest to investigate the response of the *numerical* filter F_N defined by

$$F_N = \Sigma_N^*\Sigma.$$

This question has been considered by Van Isacker and Struyleert, who showed that

$$F_N\{\, e^{i\omega t}\} = H_N(\omega)\cdot e_N^{i\omega t}$$

where the response function H_N is given by

$$H_N(\omega) = 1/[1+(i\omega/\gamma)^N]. \qquad (2\cdot 11)$$

Thus, F_N is a <u>*double action*</u> filter: it damps the input function $e^{i\omega t}$ by $H_N(\omega)$, but also truncates the Taylor series expansion at N terms. Graphs of the response function $H_N(\omega)$ for various values of N are shown in Figure 2.

The operator F_N leeves the function $e_N^{i\omega t}$ unchanged. Thus, it is idempotent of order two. However, since it is not bounded (in the supremum or L_∞ norm) it is not a projection in the Hilbert space sense.

<u>*2c. Stability*</u>

We consider the stability properties of the Laplace transform method by applying it to a simple linear oscillation equation, first with all terms transformed explicitly, and then with a term held constant during each timestep and representing the nonlinear advection.

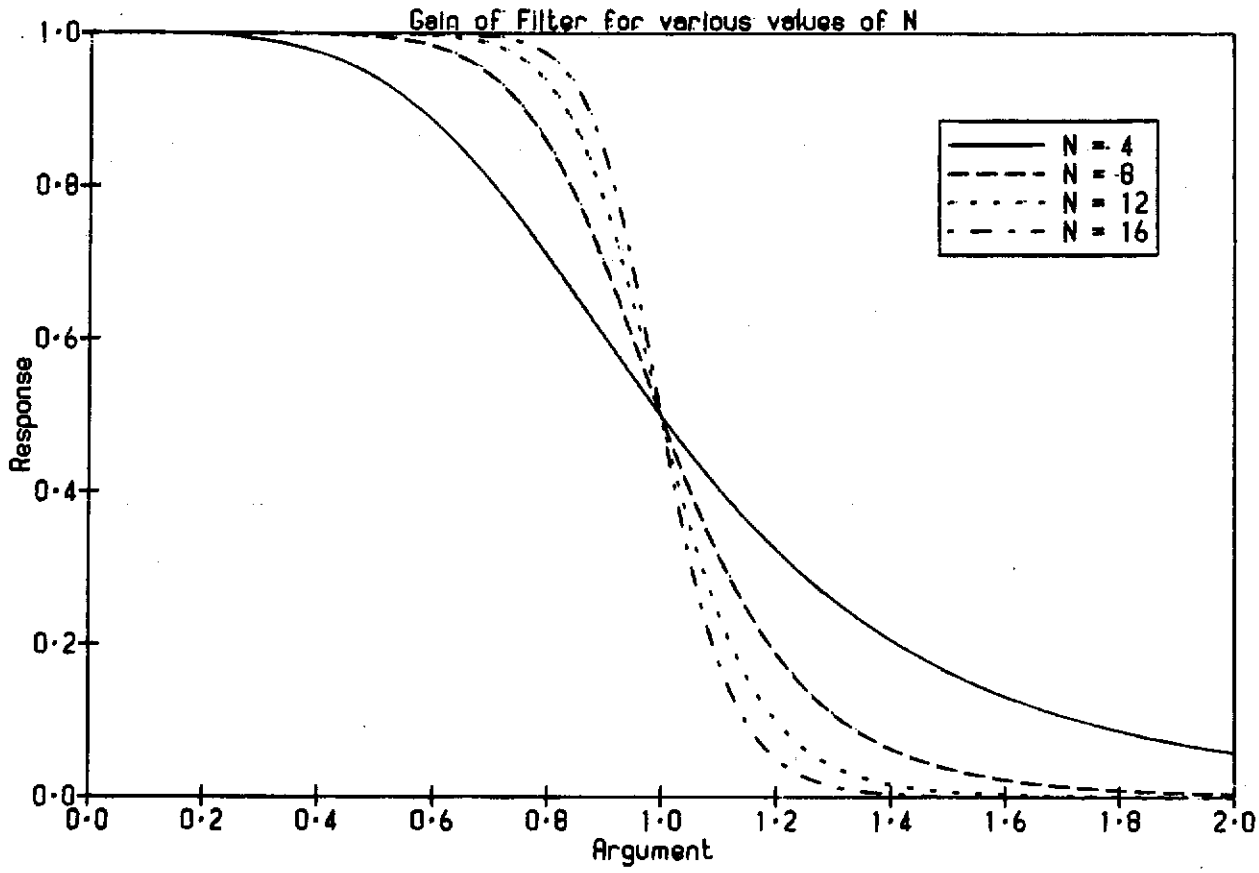
Gain of Filter for various values of N
N = 4
N = 8
N = 12
N = 16
Response
Argument
1·0
0·8
0·6
0·4
0·2
0·0
0·0
0·2
0·4
0·6
0·8
1·0
1·2
1·4
1·6
1·8
2·0

Figure 2.

Consider the oscillation equation

$$\dot{X} + i\omega X = 0, \quad X(0) = X^0 \tag{2·12}$$

Let $X^{n-1} = X((n-1)\Delta t)$ and $X^n = X(n\Delta t)$. We use the leapfrog method described in section 2a to integrate this equation. Transforming the equation with the origin of time taken at $t = (n-1)\Delta t$ we have

$$\hat{X} = X^{n-1}/(s+i\omega) \tag{2·13}$$

Then, applying the (continuous) inversion operator Σ^* with $t = 2\Delta t$ we get

$$X^{n+1} = \begin{cases} e^{-i\omega 2\Delta t} X^{n-1}, & |\omega| < \gamma \\ 0, & |\omega| > \gamma \end{cases}$$

Since $|e^{-i\omega 2\Delta t}| = 1$, we have unconditional stability, *i.e.* for the continuous operator Σ^* the timestep Δt is unrestricted. In reality we must replace Σ^* by Σ_N^*. Recall that

$$\Sigma_N^*\{ 1/(s+i\omega) \} = H_N(\omega) \cdot e_N^{-i\omega t}.$$

Thus, applying Σ_N^* to (2·13) with $t = 2\Delta t$ we get the numerical solution

$$X^{n+1} = H_N(\omega) \cdot e_N^{-i\omega 2\Delta t} \cdot X^{n-1} \tag{2·14}$$

For stability it is sufficient that the quantity multiplying X^{n-1} have modulus not greater than unity, *i.e.*

$$\left| H_N(\omega) \cdot e_N^{-i\omega 2\Delta t} \right| \leq 1 \tag{2·15}$$

Now, using Taylor's theorem with remainder we can show that

$$\left| e_N^{-i\omega 2\Delta t} \right| \leq 1 + |\omega \cdot 2\Delta t|^N / N!$$

and since the response function H_N is given by (2·11), we get, as a sufficient condition for stability, that $(\omega \cdot 2\Delta t)^N / N! \leq (\omega/\gamma)^N$, or

$$\boxed{\Delta t \leq \frac{(N!)^{1/N}}{2\gamma}} \qquad (2\cdot16)$$

Defining the cutoff period $\tau_0 = 2\pi/\gamma$, and using Stirling's formula, we may write (2·16) in a simpler, though slightly less sharp, form:

$$\Delta t \leq N\tau_0/4\pi e. \qquad (2\cdot17)$$

This is a very lenient stability criterion; for example, with typical values $N = 8$ and $\tau_0 = 12$ hours it implies

$$\Delta t \leq 24/\pi e \doteq 2\cdot8 \text{ hours}.$$

This is a longer timestep than we are likely to wish to use in practice.

If the two-step scheme is used instead of the leapfrog scheme, the permissible timestep for linear stability is doubled. Note that, in any case, this stability criterion does not depend upon the spatial resolution; this is particularly important for variable grids, where a locally fine resolution might otherwise impose an over-restrictive CFL criterion.

The advection terms impose a more stringent limitation upon the timestep. Consider (2·12) again on the interval $(0, 2\Delta t)$ and evaluate the second term at time Δt. Then the transform may be written

$$s\hat{X} = X^0 - i\omega X^1 s$$

If we invert this by applying $\sum^*$ with $t = 2\Delta t$ and assume that $X^n = A^n X^0$ we get

$$A^2 + 2i(\omega\Delta t)A - 1 = 0$$

It is straightforward to show that the roots of this quadratic for A are unimodular provided that

$$\omega\Delta t \leq 1 \qquad (2\cdot18)$$

whereas one of the roots has modulus greater than unity if this condition is violated. Thus, (2·18) is the condition for stability. The advection term is of the form $\bar{u}X_x$, which for wavenumber k and grid distance Δx becomes

$$i\left(\frac{\sin k\Delta x}{\Delta x}\right)\bar{u}X = i\omega X.$$

Therefore, stability is ensured provided we have

$$\boxed{\frac{\bar{u}\Delta t}{\Delta x} \leq 1} \qquad (2\cdot19)$$

This is the usual CFL criterion, just as we have for the semi-implicit method where advection is treated explicitly.

In the integrations we found that the leapfrog scheme remained stable provided that (2·19) was satisfied. However, the two step method became unstable if $\bar{u}\Delta t/\Delta x$ was greater than about 0·35. The reason for this is not precisely understood, but presumably it is due to the uncentered nature of (2· 6b). The results presented below are for runs using the leapfrog scheme.

It is not possible to explicitly transform the nonlinear terms. However, the CFL restriction may be circumvented in another way: the advection may be integrated by the semi-Lagrangian technique, which is unconditionally stable. In that case the only restriction is that due to the discretization of the Laplace transform, namely (2·16) above.

2d. The Forecast Model

The model used in this study is the simple one-dimensional model DYNAMO described in Lynch (1984). The basic equations may be written:

$$\zeta_t + (u\zeta)_x + f\delta + \beta v = 0 \qquad (2\cdot20)$$

$$\delta_t + (u\delta)_x - f\zeta + \beta u' + \Phi_{xx} = 0 \qquad (2\cdot21)$$

$$\Phi_t + (u\Phi)_x - f\bar{u}v + \bar{\Phi}\delta = 0 \qquad (2\cdot22)$$

The variables ζ, δ and Φ are specified on a staggered grid of M points, and periodic boundary conditions are assumed. Thus, the state of the system at any time is completely defined by the vector

$$\mathbf{X} = (\zeta_1, \delta_1, \Phi_1, \cdots, \zeta_m, \delta_m, \Phi_m, \cdots, \zeta_M, \delta_M, \Phi_M)$$

The Laplace transform of $\mathbf{X}$ is written $\hat{\mathbf{X}}$. When the system (2·20)-(2·22) is transformed, the resulting equations may be written as a single vector equation:

$$\mathbf{M}\hat{\mathbf{X}} + \hat{\mathbf{N}} = \mathbf{X}^0 \qquad (2\cdot23)$$

where $\mathbf{M}$ is a matrix depending on s, $\mathbf{N}$ is the vector of nonlinear terms and $\mathbf{X}^0$ is formed from the initial values (for more details see Lynch, 1984). Equation (2·23) is formally identical to (2·2), so that the method of integration outlined in section 2a may now be applied.

In the model runs described below we chose a channel length $L = 10^7\, m$, where $M\cdot\Delta x = L$ with $M = 50$ and $\Delta x = 200\, km$. For the chosen parameter values the maximum Rossby wave frequency and minimum gravity wave frequency have the (nondimensional) values:

$$|\nu_R|_{max} = 0.203 \quad ; \quad |\nu_G|_{min} = 2.224.$$

Any value of ν lying between these values should serve to separate the timescales. The value $\nu = 1$ was chosen. The contour $\mathbf{C}^*$ was approximated by an octogon $\mathbf{C}^*_8$ (Figure 1); only the upper half of this contour need be considered

(Lynch, 1985b). The matrix **M** was evaluated at the centre points s_n of the four upper edges Δs_n, inverted and stored for use during the forecast. The forecasts were evaluated by reference to a run using an Adams Bashforth time scheme with $\Delta t = 30$ sec., from which the rms differences in vorticity, divergence and geopotential were calculated.

3. NUMERICAL RESULTS

3a. *Comparison between the Laplace Transform (LT) and Adams Bashforth (AB) Timestepping Schemes*

In order to show that the Laplace transform (LT) scheme described above is an effective method of integrating the equations of motion, we incorporated it into the model DYNAMO (Lynch, 1984) and compared the results to those using the well-tried Adams Bashforth (AB) method.

The parameter values chosen for the parallel runs are as follows:

Gridpoints	50	Forecast Length	48 hours
Channel Length	10,000 *km*	Timestep (LT)	1 hour
Gridlength	200 *km*	Timestep (AB)	30 secs.

The initial conditions consisted of a superposition of ten wave components with randomly chosen phases and amplitudes such that the energy spectrum was proportional to $k^{-5/3}$, where k is the wavenumber. The wind was derived using the geostrophic relationship, and then the fields were initialized using the Laplace transform technique (Lynch, 1985a). The value $\gamma = 1.0$ was chosen, corresponding to a cutoff of components with periods less than 12 hours. (A modification of the iteration procedure was proposed by Vanlsacker and Struyleert (1985); this results in improved convergence properties of the scheme and was incorporated in the version used in this study). Parallel runs of the model using the LT and AB schemes were made, and the results written to disk for subsequent analysis. The root mean square (rms) values of the differences between the geopotential, vorticity and divergence fields for the two runs were calculated. The initial geopotential field (nondimensionalized) is shown in Figure 3(a), and the 48 hour forecasts using the AB and LT schemes in Figure 3(b). The two forecasts are virtually identical: the rms difference is $\sigma_\phi = 15\ m^2 s^{-2}$; this is minute compared to the standard deviation of the fields (which is of order $10^4\ m^2 s^{-2}$). The two curves of forecast geopotential in

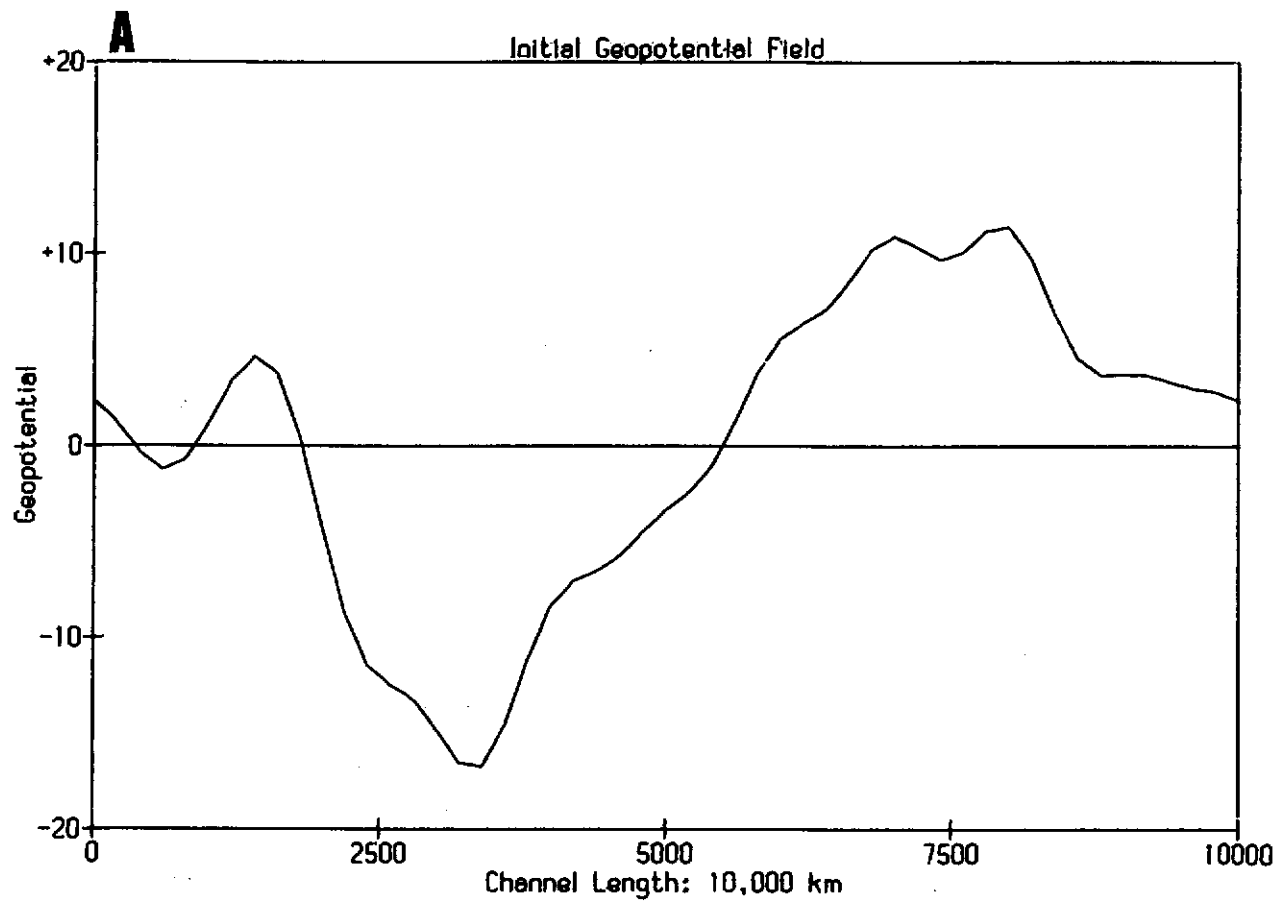
A
Initial Geopotential Field
+20
+10
0
-10
-20
Geopotential
0
2500
5000
7500
10000
Channel Length: 10,000 km

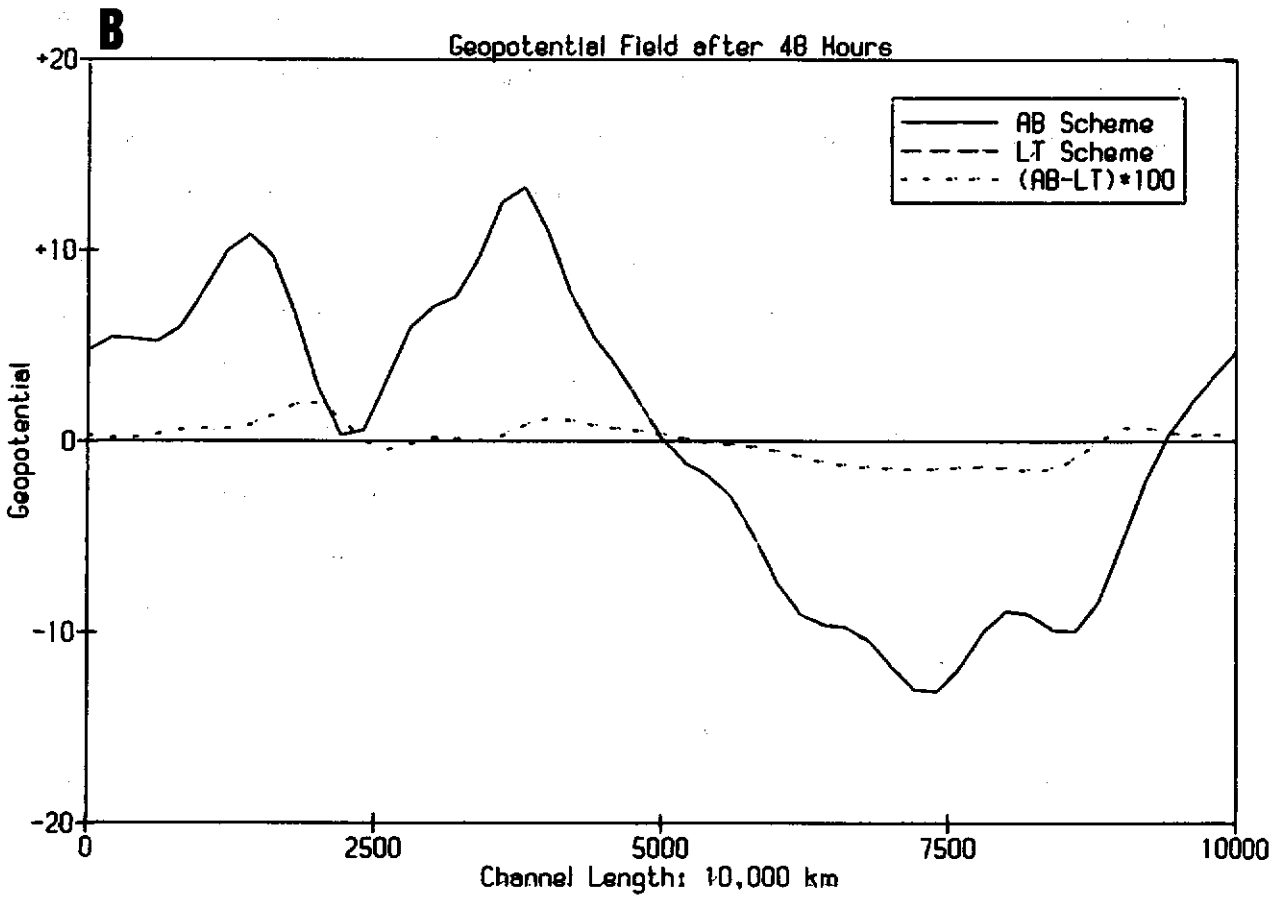
B
Geopotential Field after 48 Hours
AB Scheme
LT Scheme
(AB-LT)*100
+20
+10
0
-10
-20
Geopotential
0
2500
5000
7500
10000
Channel Length: 10,000 km

Figure 3.

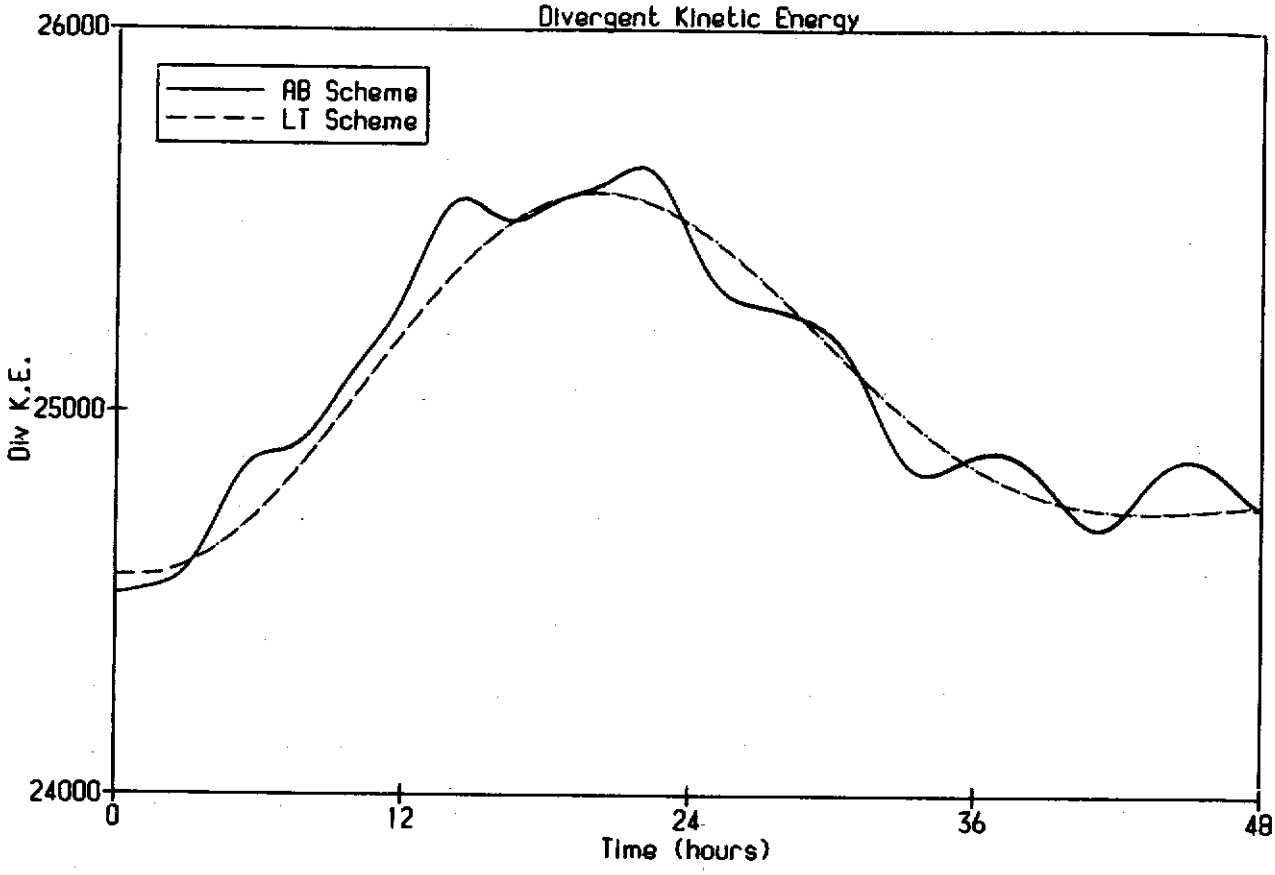

Figure 4.

TABLE 1

Root Mean Square differences of the Geopotential, Vorticity and Divergence fields, between the Adams-Bashforth (AB) run ($\Delta t = 30 sec.$) and the Laplace Transform (LT) runs with various timesteps.

Δt	σ_ϕ	σ_ζ	σ_δ
½ hr.	1.0×10^{1}	5.0×10^{-7}	1.7×10^{-8}
1 hr.	1.5×10^{1}	1.0×10^{-6}	2.0×10^{-8}
2 hrs.	2.0×10^{1}	2.0×10^{-6}	3.0×10^{-8}

Figure 3(b) are indistinguishable; a plot of the difference, scaled by 100, is also shown.

Although the geopotential forecasts are almost identical, there are some visible differences in the manner in which the divergence fields evolve in the two cases. In Figure 4 we show the divergent kinetic energy at a central point during the 48 hour run. The AB run (solid line) is noticeably noiser than the LT run (dashed line). The Laplace transform method is better at controlling gravity wave noise during the forecast. However, it should be observed that the noise in the AB run is of small amplitude and unlikely to be of significance — this is so since the fields have been well initialized.

In Table 1 we show the rms difference between the geopotential, vorticity and divergence fields, after 48 hours, of the reference run (AB scheme, $\Delta t = 30$ *sec.*) and the LT scheme with various timesteps. We can see that even with a 2 hour timestep the LT scheme yields results very close to the reference run. This implies the possibility that it may provide a very efficient means of integrating the equations of motion.

3b. *Experiments with Data Insertion during the Run*

Parallel runs to 48 hours were made with the AB and LT schemes. In each case the fields were perturbed after 12 hours in the following way: a small increment $\Delta\Phi$ is added to the Φ field and a corresponding geostrophically balanced increment is added to the meridional wind field. The integration is continued by making a forward step of length $\Delta t/2$, followed by normal centered steps. The Φ field at 12 hours, and the perturbation $\Delta\Phi$ are shown in Figure 5(a). The meridional wind field and perturbation are shown in Figure 5(b). The perturbation is meant to simulate the insertion of observational information during the forecast run. The subsequent evolution is then examined.

In the case of the AB scheme the data insertion results in the generation of noise in the ensuing forecast. This is due to the disruption of the delicate balance between the mass and wind fields. The divergent kinetic energy of the original run is plotted as a solid curve in Figure 6(a), and the results for the run perturbed after 12 hours is shown by the dashed curve.

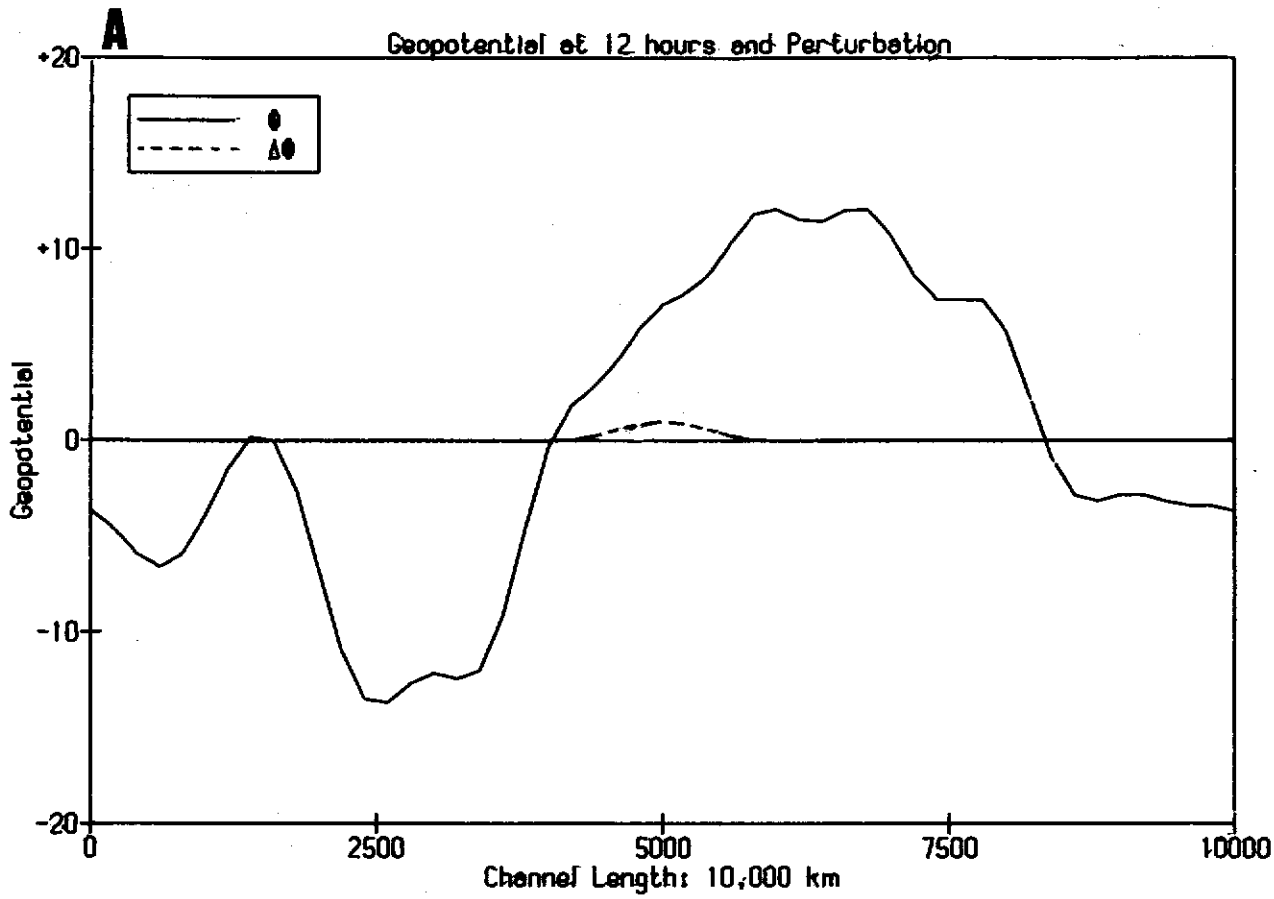
A
Geopotential at 12 hours and Perturbation
Φ
ΔΦ
+20
+10
0
-10
-20
Geopotential
0
2500
5000
7500
10000
Channel Length: 10,000 km

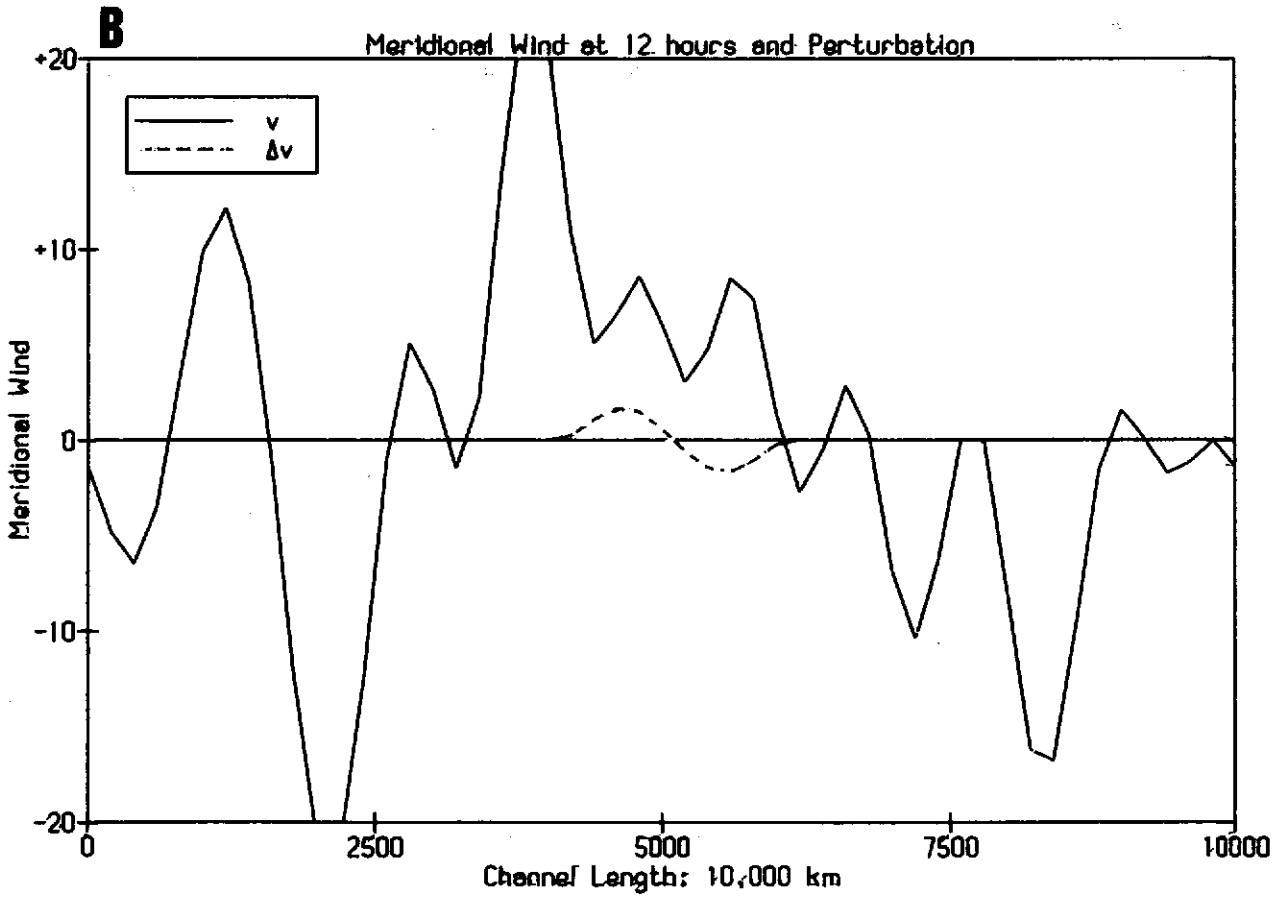
B
Meridional Wind at 12 hours and Perturbation
v
Δv
+20
+10
0
-10
-20
Meridional Wind
0
2500
5000
7500
10000
Channel Length: 10,000 km

Figure 5.

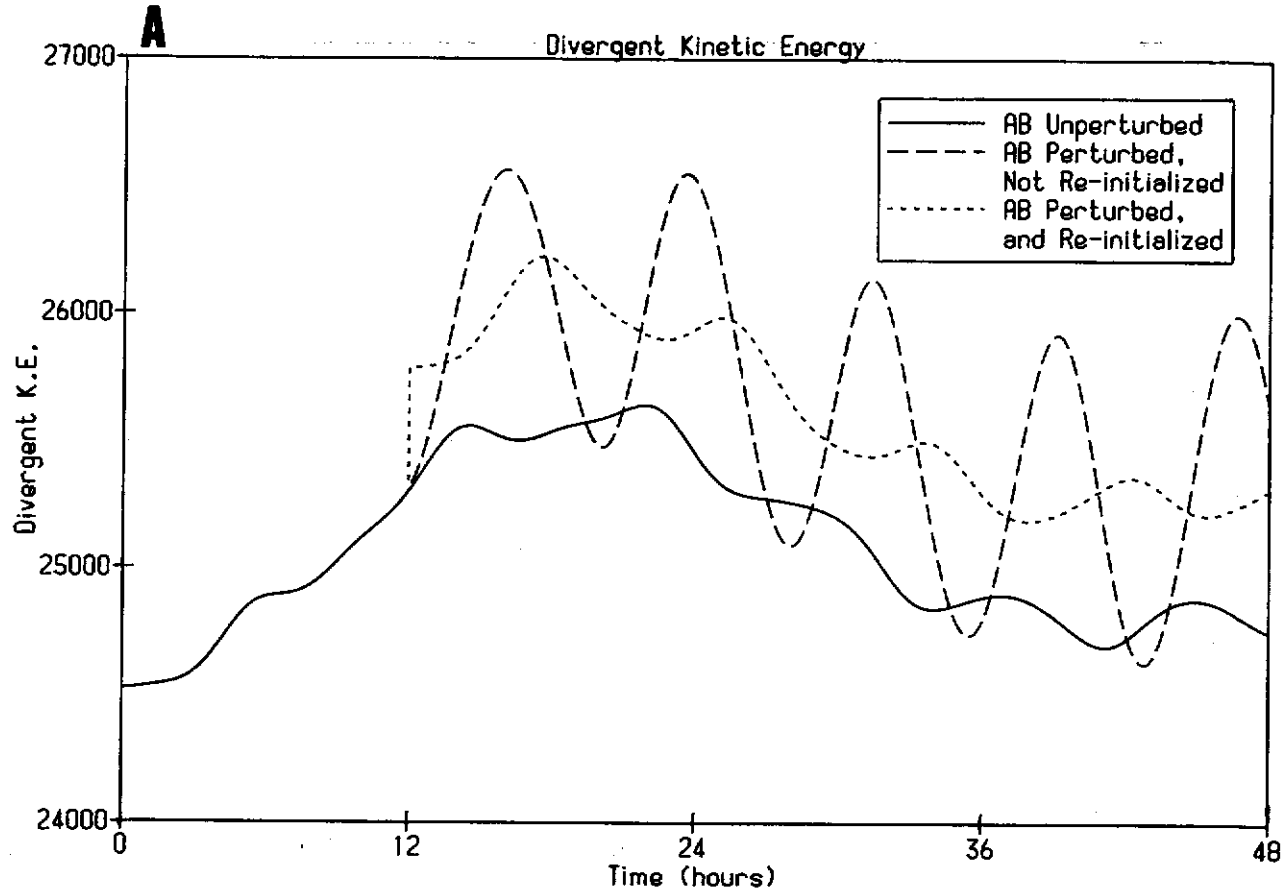
A
Divergent Kinetic Energy
AB Unperturbed
AB Perturbed, Not Re-initialized
AB Perturbed, and Re-initialized
27000
26000
25000
24000
Divergent K.E.
0
12
24
36
48
Time (hours)

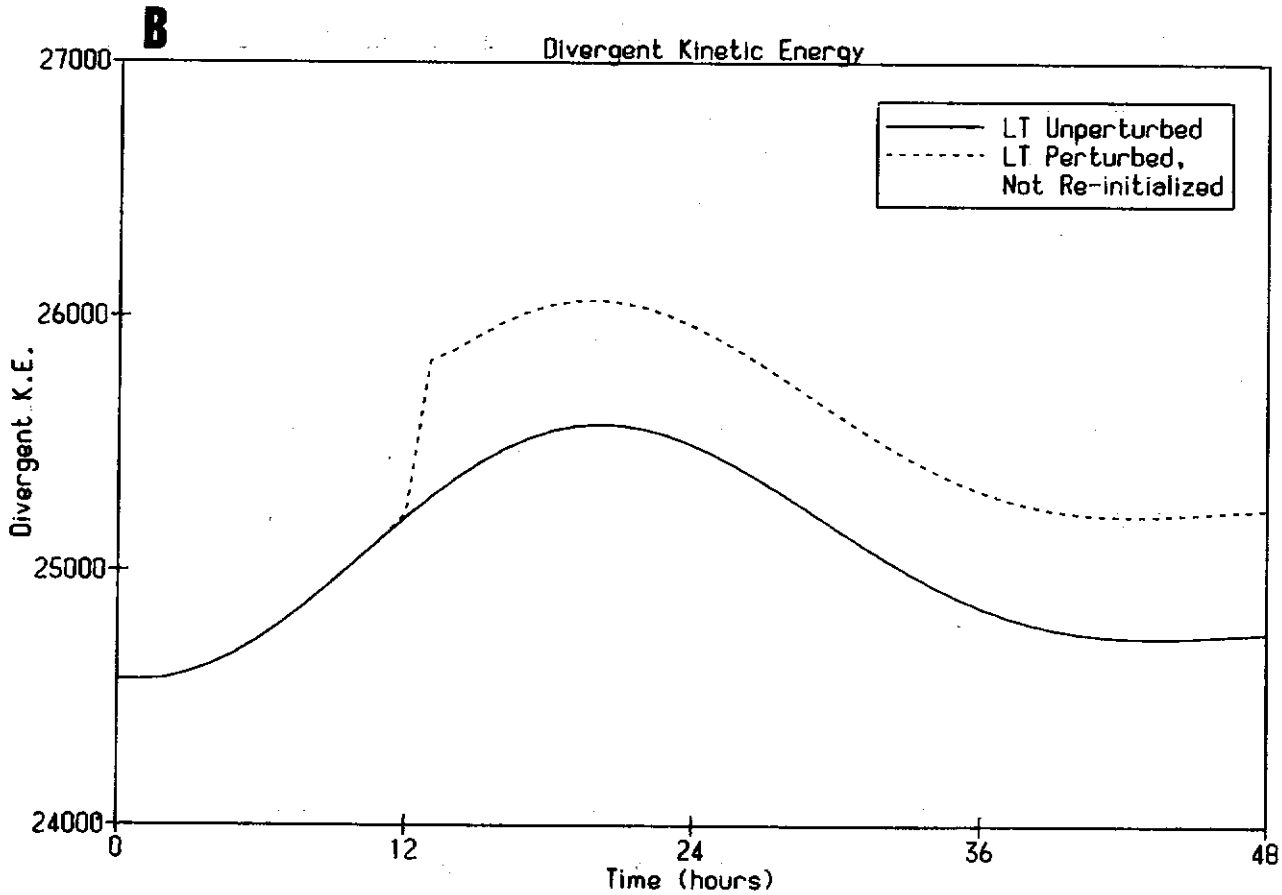
B
Divergent Kinetic Energy
LT Unperturbed
LT Perturbed, Not Re-initialized
27000
26000
25000
24000
Divergent K.E.
0
12
24
36
48
Time (hours)

Figure 6.

The system clearly suffers shock due to the insertion of the data, and the forecast is noisy thereafter. The corresponding plot of the results using fields which were *re-initialized* after data insertion is also shown (Figure 6(a), dotted line). The shock due to data insertion is much reduced, but there is still some noise remaining.

In Figure 6(b) we show the difference between the original and perturbed runs using the LT scheme. In this case the fields were <u>not</u> re-initialized after data insertion; nevertheless, there is no evidence of shock. The model forecast adjusts immediately to the new field values, and the subsequent evolution is noise-free.

The rms differences between the original and perturbed forecast fields were calculated and compared. In Figure 7(a) the differences in the geopotential field are shown. The runs are broadly similar, but there is clearly more noise in the runs using the AB scheme, even when reinitialized after data insertion. The vorticity fields, shown in Figure 7(b), are all fairly similar. Finally, in Figure 8 we see plots of the divergence fields. The shock due to the data insertion is manifest (Figure 8(a), solid line). This is reduced, but not entirely, by reinitialization (dashed line, Figures 8(a) and 8(b)). That the Laplace transform scheme can absorb the inserted data smoothly is clearly shown in the dotted curve in Figure 8(b) (note the expanded vertical scale).

The above results show that the LT scheme is capable of absorbing new observational information during the forecast run, without undue shock or noise in the ensuing forecast. The AB scheme suffers from acute noise due to data assimilation, and this is not entirely eliminated by re-initializion of the fields.

Several parallel runs were made with the AB and LT schemes, in which the fields were modified frequently during the runs, to simulate continuous data assimilation. In some cases dozens of 'observations' were introduced. The results confirmed the above findings: the LT integration proceded smoothly, adjusting to a new state of slow evolution whenever new data were introduced, whereas the AB scheme was incapable of assimilating the data without shocks.

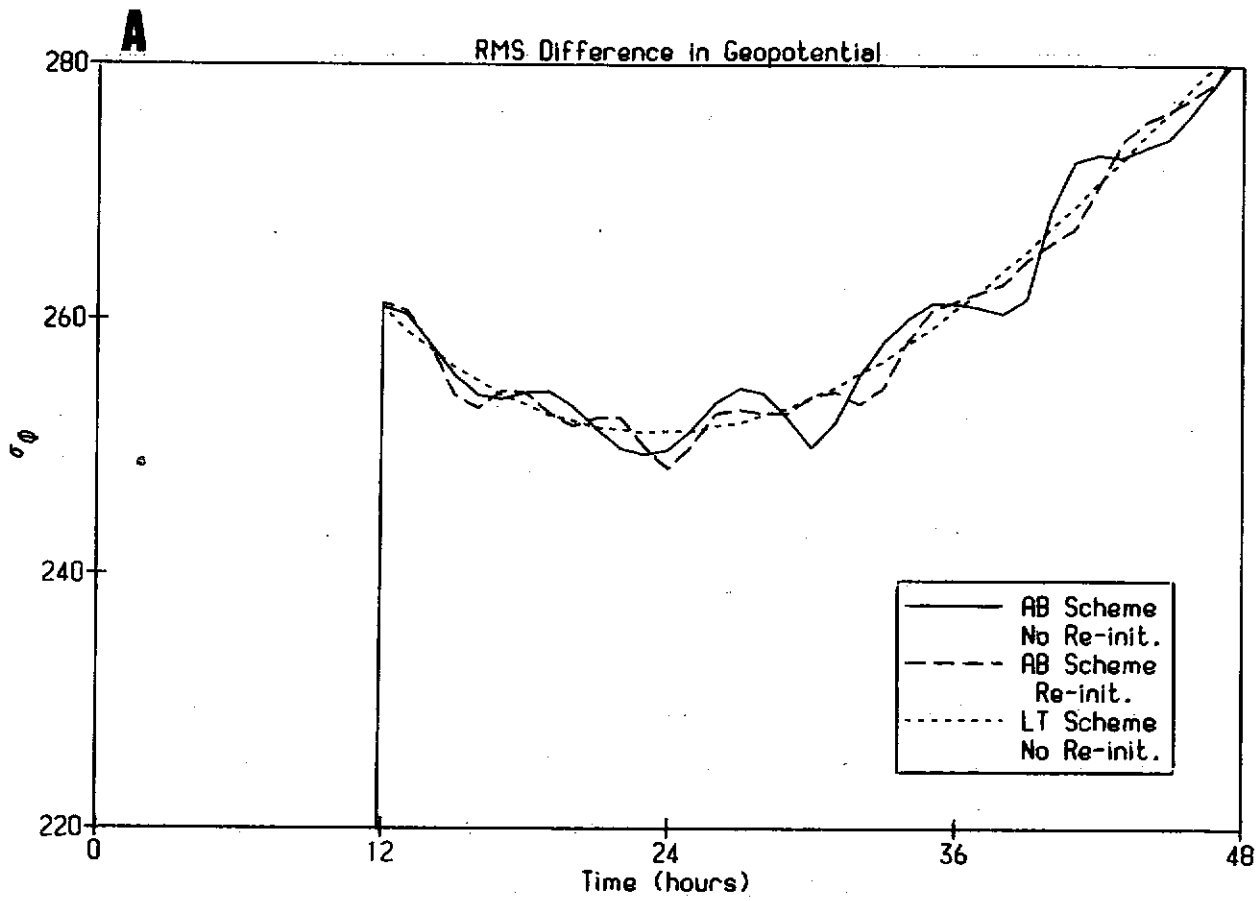
A
RMS Difference in Geopotential
280
260
240
220
σ_ϕ
0
12
24
36
48
Time (hours)
AB Scheme
No Re-init.
AB Scheme
Re-init.
LT Scheme
No Re-init.

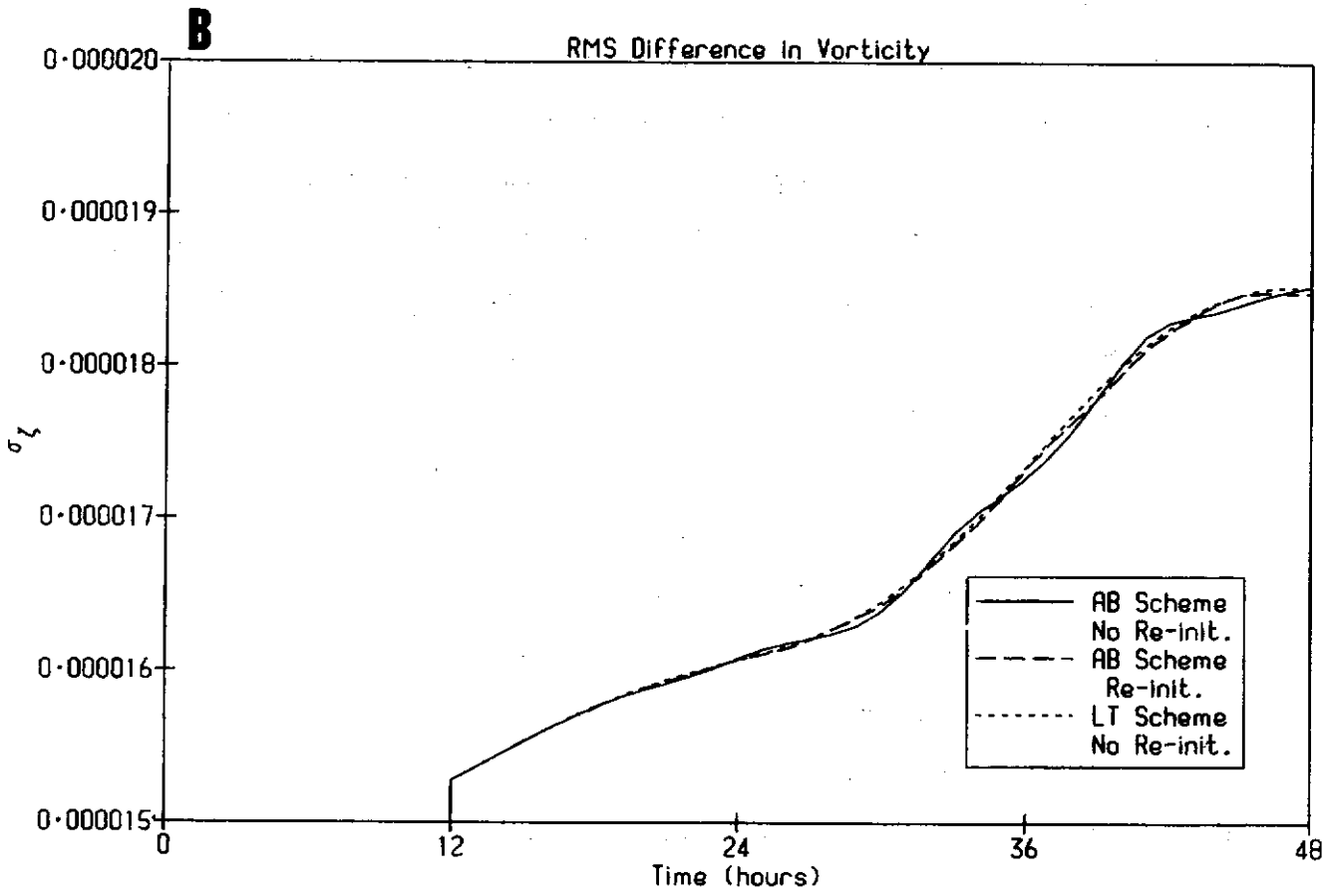
B
RMS Difference in Vorticity
0·000020
0·000019
0·000018
0·000017
0·000016
0·000015
σ_ζ
0
12
24
36
48
Time (hours)
AB Scheme
No Re-init.
AB Scheme
Re-init.
LT Scheme
No Re-init.

Figure 7.

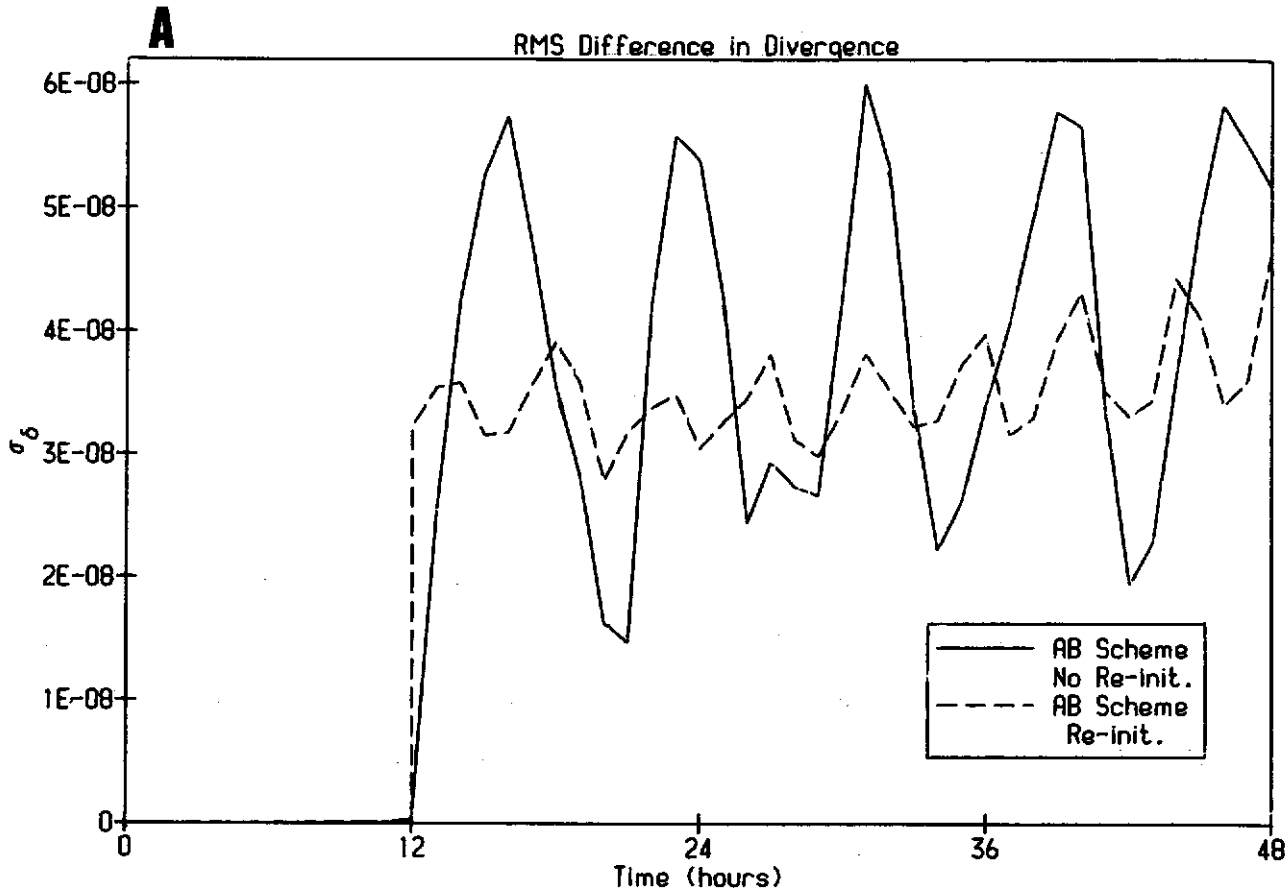
A
RMS Difference in Divergence
6E-08
5E-08
4E-08
3E-08
2E-08
1E-08
0
σ_δ
0
12
24
36
48
Time (hours)
AB Scheme
No Re-init.
AB Scheme
Re-init.

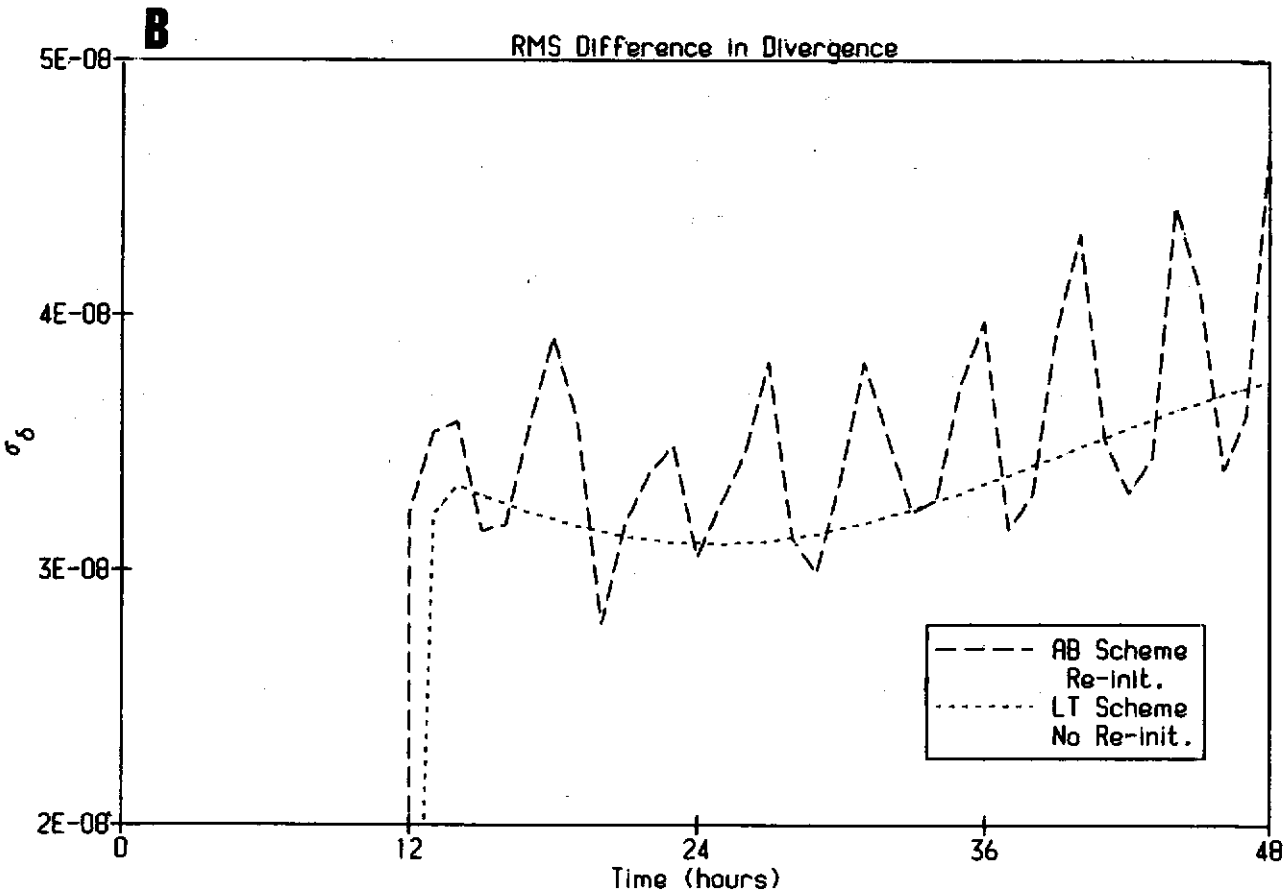
B
RMS Difference in Divergence
5E-08
4E-08
3E-08
2E-08
σ_δ
0
12
24
36
48
Time (hours)
AB Scheme
Re-init.
LT Scheme
No Re-init.

Figure 8.

4. THE LAGRANGIAN ADVECTION SCHEME

The LT scheme handles the linear terms in such a manner as to allow a large timestep; the only restriction, due to the discretization of the inversion integral, is a very lenient one (2·16). This means that the fast gravity waves do not limit the timestep. However, the nonlinear advection terms are handled in an explicit manner, and this results in a CFL criterion depending on the advection speed (2·19). For realistic atmospheric flows this limitation can be problematic, as the advective windspeed may be locally large. A means of circumventing this restriction is to use a Lagrangian scheme for advection (Robert, 1981; Bates and McDonald, 1982).

To test the above idea the model was modified in such a way that the advection by the mean flow $\bar{u}$ was integrated in a Lagrangian manner. Thus, we have, for example,

$$\Phi_k^{n+1} = \Phi_*^{n-1}$$

such that the value at gridpoint k at time $(n+1)\Delta t$ equals the value at some departure point (denoted by the star) at time $(n-1)\Delta t$. The departure point is a distance $2\bar{u}\Delta t$ upstream from the gridpoint k and the variables are evaluated there by quartic interpolation (using the nearest five gridpoints). The source term $(-f\bar{u}v = v\bar{\Phi}_y)$ is also an advective term and was integrated in a Lagrangian manner; however, in order to avoid spurious energy generation it was found to be necessary to use the meridional velocity at the arrival point in calculating this term. We discuss this further below.

Each advection step was followed by an adjustment step which used the Laplace transform technique to integrate the remaining terms. We call the combined scheme the Laplace-Lagrange (LL) model.

Three parallel runs were made using the Adams Bashforth (AB) scheme, the Laplace transform (LT) method with the advection terms

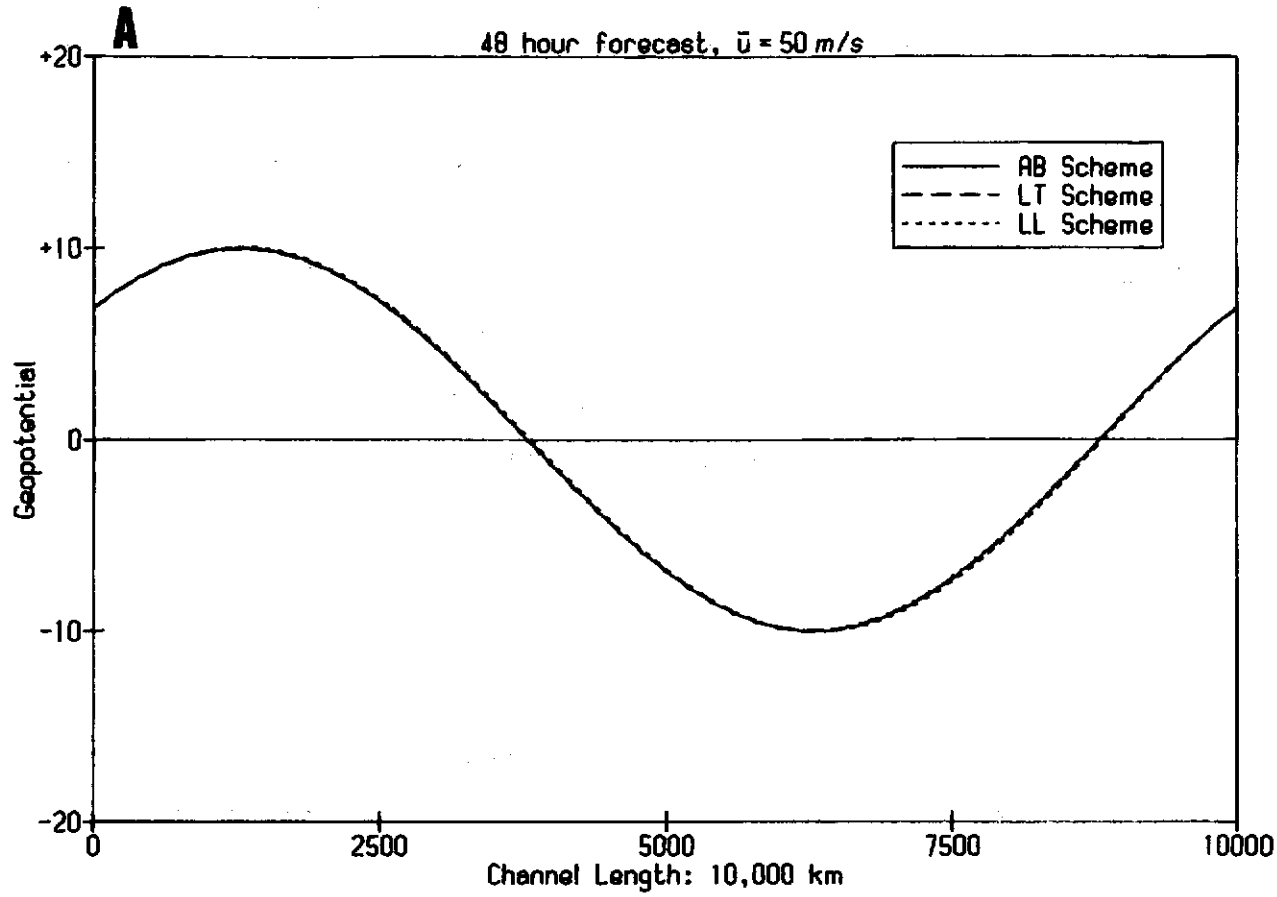
A
48 hour forecast, ū = 50 m/s
AB Scheme
LT Scheme
LL Scheme
+20
+10
0
-10
-20
Geopotential
0
2500
5000
7500
10000
Channel Length: 10,000 km

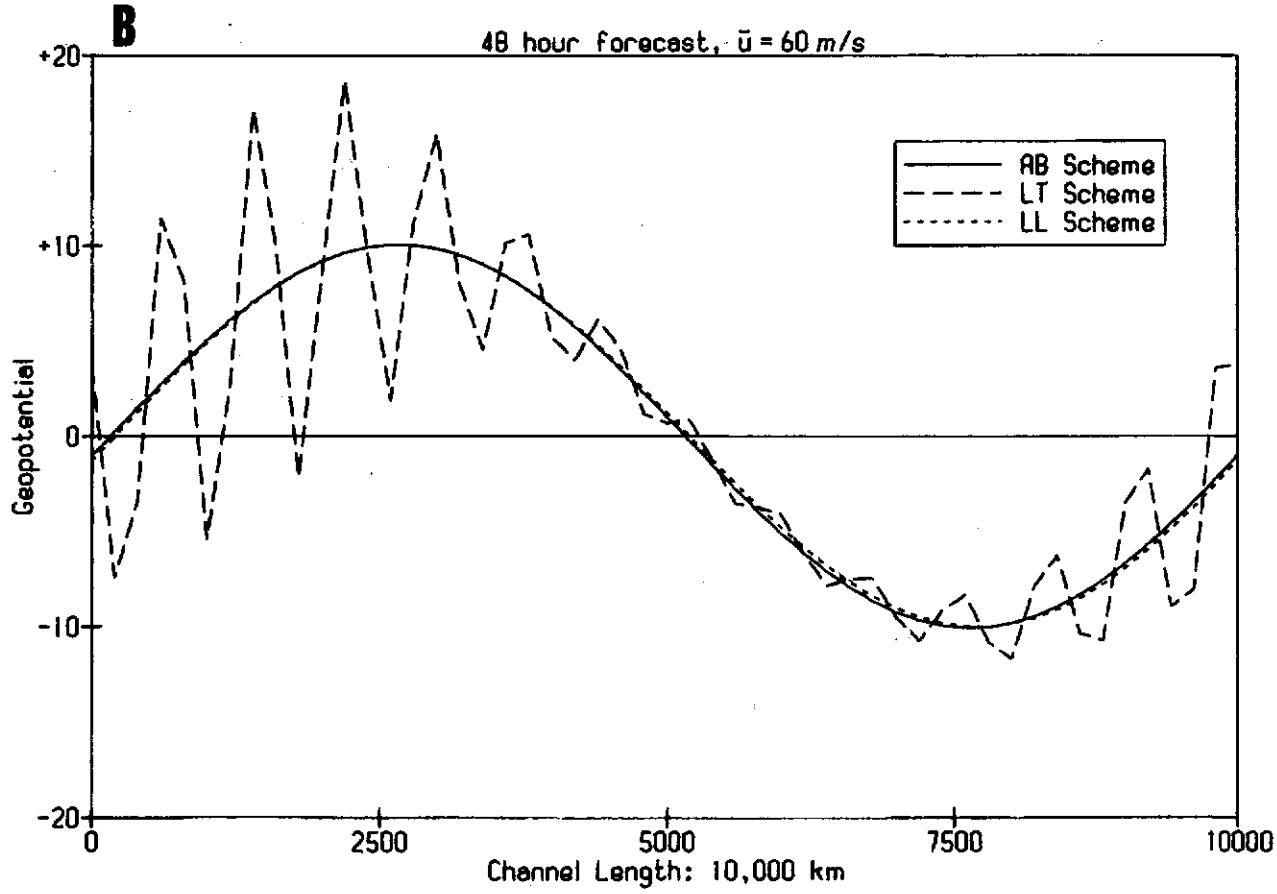
B
48 hour forecast, ū = 60 m/s
AB Scheme
LT Scheme
LL Scheme
+20
+10
0
-10
-20
Geopotential
0
2500
5000
7500
10000
Channel Length: 10,000 km

Figure 9.

integrated explicitly, and the Laplace-Lagrange (LL) scheme described above. The initial condition was a geostrophically balanced wavenumber one perturbation superimposed on a zonal mean flow $\bar{u}$. The stability of the LT scheme is determined by the nondimensional number $Le = \bar{u}\Delta t/\Delta x$ (denoted Le for Lewy, who discovered the stability criterion (see Reid, 1976, p116)). For the AB scheme we set $\Delta t = 30\,sec.$, and for the LT and LL runs $\Delta t = 3600\,sec. = 1$ hour. The grid interval was $\Delta x = 200\,km$ in all cases. Thus, the critical velocity for stability is $\bar{u} = 55{\cdot}5^{*}\ m\,s^{-1}$. We chose two values of the zonal velocity as follows:

$$\bar{u} = 50\ m\,s^{-1} \quad ; \quad Le = 0{\cdot}90$$
$$\bar{u} = 60\ m\,s^{-1} \quad ; \quad Le = 1{\cdot}08$$

The forecast geopotential after 48 hours is shown in Figure 9. For $\bar{u} = 50\,m/s$ the three schemes give very similar results — it is difficult to distinguish between the three curves in Figure 9(a). For $\bar{u} = 60\,m/s$ the stability criterion ($Le < 1$) is violated and the LT scheme becomes unstable. This is clearly seen in Figure 9(b). The Adams Bashforth and Laplace-Lagrange schemes remain stable, and both give very similar results — the AB and LL curves are almost identical.

Further runs with $\bar{u} = 100\,m/s$ and with other initial conditions confirmed that the LL scheme remains stable for strong advection. This scheme gives us a method of integrating the equations using timesteps of the order of an hour, without the problem of numerical instability. The only restriction is the criterion (2·16) due to the discretization of the inversion integral.

In the case where all three schemes remained stable the errors in the LL scheme, though small, were larger than those using the LT scheme (errors were relative to the AB run). This is believed to be due to the handling of the source term ($-f\bar{u}v$). In the case of geostrophic flow this term exactly balances the mean advection $\bar{u}\Phi_x$, and in general it seems that special care must be taken in modelling the small residual. The results with the LL scheme were found to be quite sensitive to the precise manner in which this term was integrated. The question was not examined further, since in more general models the advection is not separated into components in this way.

5. DISCUSSION

The numerical technique discussed in this report allows us to forecast the meteorologically significant components of the flow whilst attenuating the high frequency components to the level necessary for nonlinear balance of the rotational modes. The application of the method does not require explicit knowledge of the normal modes of the forecast model.

Van Isacker and Struylaert (1985) have applied the Laplace transform method to a three dimensional global spectral model. They report that the method provides an efficient means of integrating the primitive equations, allowing them to use a large timestep, and that the evolution of the meteorological fields is much smoother that that obtained using explicit integration methods.

Daley (1980) has used the ideas of normal mode initialization to develop a method of integrating the primitive equations efficiently. The original equations can be written

$$\dot{\mathbf{X}} + \mathbf{L}\mathbf{X} + \mathbf{N}(\mathbf{X}) = \mathbf{0} \qquad (5\cdot1)$$

where $\mathbf{X}$ is the state vector of unknowns, $\mathbf{L}$ is a constant linear operator (matrix) and $\mathbf{N}$ is a nonlinear vector function. When transformed to Hough mode space, the system splits into two subsystems:

$$\dot{\mathbf{Y}} + \mathbf{A}_1\mathbf{Y} + \mathbf{N}_1(\mathbf{Y},\mathbf{Z}) = \mathbf{0} \qquad (5\cdot2)$$

$$\dot{\mathbf{Z}} + \mathbf{A}_2\mathbf{Z} + \mathbf{N}_2(\mathbf{Y},\mathbf{Z}) = \mathbf{0} \qquad (5\cdot3)$$

Where $\mathbf{Y}$ and $\mathbf{Z}$ are respectively the coefficients of the slow and fast components of the flow and $\mathbf{A}_1$, $\mathbf{A}_2$ are diagonal matrices of eigenfrequencies. Assuming Machenhauer's criterion ($\dot{\mathbf{Z}} = \mathbf{0}$) to hold throughout the integration, Daley replaced (5·2)-(5·3) by the system

$$\dot{Y} + A_1 Y + N_1(Y,Z) = 0 \qquad (5\cdot4)$$

$$A_2 Z + N_2(Y,Z) = 0 \qquad (5\cdot5)$$

giving a prognostic equation for the slow modes and a diagnostic equation for the fast modes. I will call (5·4)-(5·5) the *Slow Equations.* Using the slow equations, Daley developed an integration scheme which was stable, efficient and accurate: he compared a run with the slow equations and $\Delta t = 40$ min. to a control run with the primitive equations and $\Delta t = 10$ min.; the rms differences in surface pressure and 500 hPa winds at 48 hours were only 0·6 hPa and 1 m/s. These differences are minute.

The great majority of the additional computational effort (per timestep) in Daley's scheme is due to the transformations between spectral (spherical harmonic) space and normal (Hough-)mode space; for a gridpoint model the transformations would be even more expensive. The Laplace transform technique avoids these transformations but involves, instead, transformations to and from image space (s-space), which are also expensive. Using the ideas of implicit normal mode initialization (Temperton, 1985; Juvanon du Vachat, 1986), I have derived a set of equations, expressed in terms of the physical variables (not normal modes), which forecast the low frequency motions while diagnosing appropriate gravity wave components. These *slow equations in physical space* obviate the need for costly transformations. The slow equations are similar to the balance system, but not identical to it. They would appear to provide us with a means of selectively forecasting those components of the atmospheric motion which are important, while avoiding the troubles associated with the gravity waves. They would also seem to provide a suitable means for the assimilation of observational data during a forecast, as they can absorb inserted data without suffering high frequency shocks.

The three methods mentioned here are obviously all closely related to each other, and may be expected to behave similarly in their handling of gravity wave noise. All would seem to show promise in the area of continuous data assimilation. Since the slow equations in physical space require no

transformations, they would seem to offer the most attractive prospect. They involve the solution of Helmholtz and Poisson equations at each timestep and would therefore be most economically incorporated in a spectral (spherical harmonic) context. It is hoped to test the slow equations in a full baroclinic model and to present the results in a further report.

ACKNOWLEDGEMENTS

The work reported here was begun whilst I was a Visiting Scientist at the Royal Netherlands Meteorological Institute, De Bilt. I am grateful to my colleagues there for all their help and kindness. I am also grateful for the opportunity to have visited Drs. Van Isacker and Struylaert in KMI, Uccle and the HIRLAM group in Copenhagen, where Dr. Machenhauer drew my attention to the similarity between the Laplace transform approach and the normal mode forecasting method of Daley.

APPENDIX

Laplace Transform Theory

The basic definitions and properties of Laplace transforms needed in this study are summarized, and the method of filtering is described. A good comprehensive guide to the theory, from a practical viewpoint, is Doetsch (1971).

The Laplace transform of a function $f(t)$ of time t is defined as:

$$\mathcal{L}\{f(t)\} = \hat{f}(s) = \int_0^\infty f(t)e^{-st}dt \qquad \text{(A1)}$$

and is a function of the associated complex variable s. Thus, a constant a transforms to a/s. The complex exponential function representing a wavemotion is transformed to an algebraic function

$$\mathcal{L}\{e^{i\omega t}\} = 1/(s - i\omega). \qquad \text{(A2)}$$

Since $\mathcal{L}$ is linear, the superposition of a number of waves may be transformed component-wise:

$$\mathcal{L}\{\sum_{j=1}^{J} a_j e^{i\omega_j t}\} = \sum_{j=1}^{J} a_j/(s - i\omega_j). \qquad \text{(A3)}$$

The higher the frequency ω_j, the further the corresponding pole $s = i\omega_j$ lies from the origin.

If the transform of $f(t)$ is $\hat{f}(s)$ then the time-derivative, $f'(t)$, transforms as

$$\mathcal{L}\{f'(t)\} = s \cdot \hat{f}(s) - f(0) \qquad \text{(A4)}$$

where $f(0)$ is the initial value of $f(t)$. Thus, differentiating in t-space corresponds to algebraic operations in s-space. This is the power of the Laplace transform method: it lowers the level of transcendence of functions and operators. Ordinary differential equations transform to algebraic ones.

A modification of the Fourier theorem gives us the complex inversion formula for the Laplace transform:

$$f(t) = \mathcal{L}^{-1}\{\hat{f}(s)\} = \frac{1}{2\pi i}\int_C \hat{f}(s)e^{st}ds \qquad \text{(A5)}$$

where the contour C is parallel to the imaginary axis, and to the right of all singularities of $\hat{f}(s)$. We assume that $\hat{f}(s)$ is meromorphic, that is, analytic except for isolated poles; and that the contour C can be completed by an asymptotically large semicircular arc in the left half plane.

The contributions to $f(t)$ in (A5) come from the poles of $\hat{f}(s)$. Since the high-frequency components correspond to poles far from the origin, they can be eliminated by shrinking the contour to a circle C^* of radius r centered at the origin. This is the motivation for the definition of the operator $\mathcal{L}^*$ [Eq. (7), Section 2b], and we see that $\mathcal{L}^*\mathcal{L}$ acting on $f(t)$ will select the components with frequency $\omega < r$ and filter out the high-frequency components of $f(t)$.

References:

Bates, J.R. and A. McDonald, 1982: Multiply-upstream semi-Lagrangian advective schemes: analysis and application to a multi-level primitive equation model. *Mon. Weather Rev.*, **110**, 1831-1842.

Daley, R., 1980: The development of efficient time integration schemes using normal mode models. *J. Atmos. Sci.*, **108**, 100-110.

Doetsch, G., 1971: *Guide to the Applications of the Laplace and Z-Transforms*. Van Nostrand Reinhold, 240 pp.

Juvanon du Vachat, R., 1986: A general formulation of normal modes for limited area models; application to initialization. (accepted for publication, *Mon. Weather Rev.*)

Lynch, Peter, 1984: DYNAMO - A one dimensional primitive equation model. Tech. Note No. 44, Irish Meteorological Service, Dublin.

Lynch, Peter, 1985a: Initialization using Laplace Transforms. *Q. J. Roy. Met. Soc.*, 111, 243-258.

Lynch, Peter, 1985b: Initialization of a Barotropic Limited-Area Model using the Laplace Transform Technique. *Mon. Weather Rev.*, **113**, 1338-1344.

Machenhauer, B., 1977: On the dynamics of gravity oscillations in a shallow water model, with applications to normal mode initialization. *Beitr. Phys. Atmos.*, **50**, 253-271.

Reid, C., 1976: *Courant in Göttingen and New York*. Springer-Verlag, New York, Heidelberg, Berlin.

Robert, A., 1981: A stable numerical integration scheme for the primitive meteorological equations. *Atmos.-Ocean*, **19**, 35-46.

Temperton, C., 1985: Applications of a new principle for normal mode initialization. Preprint Volume, Seventh Conference on Numerical Weather Prediction, June 17-20 1985, Montreal, P.Q., American Meteorological Society, Boston, Mass.

Van Isacker, J. and W Struylaert, 1985: Numerical Forecasting using Laplace Transforms. Roy. Belgian Met. Inst., Pub. Ser. A - No. 115.